https://doi.org/10.48048/tis.2024.7355

Estimation of Energy Separation in Tunelling States in Symmetric-Hyperbolicus Double-Well Potential Problem using Filter Method

Abdurrouf*, Gancang Saroja and Muhammad Nurhuda

Physics Department, Faculty of Mathematics and Natural Sciences, Brawijaya University, Indonesia

(*Corresponding author's e-mail: abdurrouf@ub.ac.id)

Received: 1 August 2023, Revised: 6 September 2023, Accepted: 11 September 2023, Published: 20 January 2024

Abstract

Double well potential (DWP) plays an important role in quantum physics but its analytical exact solutions are incomplete, except for some limited quasi-exact solvable (QES) and therefore numerical solutions are still required. This paper is aimed to obtain numerical solution of the recently proposed symnetric-hyperbolicus DWP $V(x)=a^2\sinh^2(x)-k\tanh^2(x)$ and $V(x)=c^2\sinh^4(x)-k\tanh^2(x)$ by using our newly developed filter method. The filter method is able to produce eigen-energies and eigenfunctions those are in accordance with the exact analytical results. Next, we obtain the dependence of the ground state energy and the energy separation between the 2 lowest states on the DWP parameter *k*. For large *k*, the 2 lowest energy levels are below the potential barrier so the eigenfunctions penetrate the barrier, so the 2 lowest energy levels can be considered as the result of a single energy split. In this case, we observe that the energy separation $\Delta E = E_2 - E_1$ is an exponential function *k*, as opposed to a linear function for smaller *k* in the non tunelling region. The exponential trend of the numerical results is in good agreement with the theoretical approach and allows one to estimate the 2 lowest energies for a given *k*.

Keywords: Classical action, Double-well potenttial, Energy separation, Filter method, Numerical solution, Splitting energy, Tunelling state

Introduction

One of the most interesting and important classes of potentials that has been studied extensively in quantum physics is the so-called double well potential (DWP). The DWP consists of 2 minima separated by a potential barrier in the middle. The 2 minima have the same shape for a symmetric DWP, and a different shape for an asymmetric DWP [1]. DWP can be used to model particle motion under 2 force centers, such as the motion of atoms P in phosphine structure which produces infrared spectroscopy [2] and motion of electrons in metals which is responsible for the metal-to-isolator transition [3]. Other physical phenomena modeled with DWP include particle tunneling under Bose-Einstein condensate conditions which produces an interesting collective effect [4,5], quantum tunneling effect when a particle can pass through a classically bounded region [6,7], and quantum computing when a multiple well potential is used to build a quantum logic gate [8]. As an example of practical application, DWP can be used to study resonant tunnel diodes [9] and control temperature-related electronic lowland states in semiconductors [10].

Among the well-known DWP models are the symmetric-hyperbolic DWP including the Razavy bistable potential (RBP) which successfully described molecular torsion oscillations with n and $2n$-fold resistance [11], the Konwent potential which successfully modeled nucleons in the nucleus [12], and the double sinh Gordon (DSHG) potential which was applied to sink and anti-sink calculations in thermodynamics [13]. Nowadays, hyperbolic DWPs are used to investigate the electrical and optical properties in semi conductor by investigating the role of structure parameters [14-16], applied external fields [17-20] and applied magnetic fields [21]. Despite having many possible applications, the solutions of symmetric-hyperbolic DWP are not complete, where quasi-exact solvable (QES) of the eigen-energies and eigenfunctions have been obtained for some limited lowest states only [11-13,22].

In order to obtain a complete solution, several attempts were made to study the nature of Heun's confluent function and explore the possibility of its application in solving DWP problems [23]. Since then, many DWPs have exactly or semi-excatly solved in the term of confluent Heun function including quartic potential [24], sextic potential [25], hyperbolic potential [26,27], RBP potential [28], Razavy cocinus potential [29], Konwent potential [30], asymmetric DWP potential [31], harmonic oscillator plus non-polynomial interaction [32] and Mathieu potential [33].

However, the use of the Heun's confluent function has a weakness because the potential must be in the specific form of the Heun's confluent function, the solutions are not always in a closed form, and simetimes the solutions can be difficult to interpret. In addition, the eigen-energy is one of the parameters needed to construct the Heun's confluent function. For this reason, a numerical solution of the Schrödinger equation for the DWP is still urgently needed. Recently, various techniques are competing, including pseudospectral methods [34], asymptotic iteration method (AIM) [35], combination of energy factorization approach and stabilization approach [36], Lagrangian description [37], fractional Schrödinger equation [38] and Hill determinant method [39].

Particles trapped in the DWP may have greater or less energy than the peak potential barrier. For a particle with an energy lower than the peak barrier potential, the particle tunnels along the barrier where it splits into 2 separate energy levels. It has been studied theoretically that the energy separation reduces exponentially by S, where S is the action in the classical forbidden region (between 2 turning points) [40,41].

In this paper, we investigate the symmetric-hyperbolic DWP proposed by Dong *et al.* [26], using our newly developed filter method [42]. While Dong *et al.* having reported the dependence of energy levels on DWP parameters, we generate more numerical solutions, including eigen-energies and eigenfunctions. By analyzing the available data, we formulate equations for the first energy level and the energy separation between the 2 lowest energy levels, as a function of the DWP parameter. We also investigate how the DWP parameter controls the energy pattern and its relationship to S action.

Materials and methods

The filter method is based on the idea that any wave packet within a defined space can be expressed as a superposition of all eigenfunction. By applying an appropriate operator, one can basically select the specific eigenfunction from the wave packet. To pick up the eigenfunction, we implement the filter operator, which is defined as [42];

$$\hat{F} = \frac{1}{\hat{H} - E_n} \tag{1}$$

where $\hat{F}$ and $\hat{H}$ stands for filter and Hamiltonian operator respectively. In Eq. (1), E_n is the eigen-energy, whose eigenfunction will be picked up. Operator $\hat{F}$ acts globally on the space, and therefore the solution of the eigenfunction is independent of the boundary-value condition and hence determined by the Hamiltonian and the eigen-energy only. Once operator $\hat{F}$ is applied to the wavefunction, it is expected that only the selected eigenfunction with $E = E_n$ survives, while other eigenfunctions whose energies are not matched, decrease.

$$\hat{F}\psi(\mathrm{r}) = \frac{1}{\hat{H} - E_n}\sum_{m=0}^{\infty} a_m\phi_m(\mathrm{r}) = \sum_{m=0}^{\infty} a_m\phi_m(\mathrm{r})\delta(E_m - E_n) = \tilde{\phi}_m^1(\mathrm{r}) \tag{2}$$

However the eigenfunction $\tilde{\phi}_m^1(\mathrm{r})$ is not a normalized function and should be normalized as follow;

$$\phi_m^1(\mathrm{r}) = \frac{\tilde{\phi}_m^1(\mathrm{r})}{\sqrt{\int d^3\mathrm{r}\left|\tilde{\phi}_m^1(\mathrm{r})\right|^2}} \tag{3}$$

Using the normalized eigenfunction, we calculate the eigen-energy as;

$$E_n^1 = \int d^3\mathrm{r}\phi_m^1(\mathrm{r})\hat{H}\phi_m^1(\mathrm{r}) \tag{4}$$

This process can be repeated for a range of energy to obtain the energy spectrum in that region. The filter method has ben succesfully applied to some single potentials [42] as well as some periodic potentials [43-46].

In this current work, the filter method is applied to solve Schrödinger equation with a class of symmetric hyperbolicus DWP [26]. In solving Schrödinger equation, we use Rydberg atomic units with $e = 2m_e = \hbar = k = 1$. The first problem is generated by potential in the form of;

$$V(x) = a^2 \sinh^2(x) - k \tanh^2(x), \tag{5}$$

where a and k are positive constants. It has been observed that the Schrödinger equation with the above potential has solution in form of Heun;s comfluent function as follow [26];

$$\psi(x) = \cosh^{(1\pm1)/2}(x) H_C(\alpha, \pm\beta; \gamma, \delta, \eta, z), \tag{6}$$

where $\tau = \sqrt{1-8k}$, $\alpha = 0$, $\beta = \frac{\tau}{2}$, $\gamma = -\frac{1}{2}$, $\delta = -\frac{a^2}{2}$, $\eta = \frac{1}{8}\left(4a^2 + 4E + 3\right)$ and $z = \cosh^2(x)$

The second problem is generated by potential in the form of;

$$V(x) = c^2 \sinh^4(x) - k \tanh^2(x), \tag{7}$$

where c and k are positive constants. It has been observed that the Schrödinger equation with the above potential has solution in form of [26];

$$\psi(x) = \exp\left(\sqrt{2}z\right)\cosh(x) H_C(\alpha, \beta; \gamma, \delta, \eta, z), \tag{8}$$

where $\tau = \sqrt{1-8k}$, $\alpha = \sqrt{2}c`$, $\beta = \frac{\tau}{2}$, $\gamma = -\frac{1}{2}$, $\delta = -\frac{c^2}{2}$, $\eta = \frac{1}{8}\left(-4c^2 + 4E + 3\right)$ and $z = \cosh^2(x)$

Results and discussion

The potential profile of Eq. (5) is depicted in **Figure 1** for constant a and various k (left panel) and for constant k and various a (right panel). It exhibits a local maximum at its center $x_{max} = 0$ with $V_{max} = 0$ and 2 symmetric local minima at $x_{min} = \pm\text{acosh}\left(\left(\frac{k}{a^2}\right)^{1/4}\right)$ with $V_{min} = -\left(a - \sqrt{k}\right)^2 < 0$. It is clear that the double-well potential appears for $k \geq a^2$ only, and is more pronounced for larger k (**Figure 1** – left panel) and/or smaller a (**Figure 1** – right panel). For $k < a^2$, Eq. (5) reduces to a single well potential.

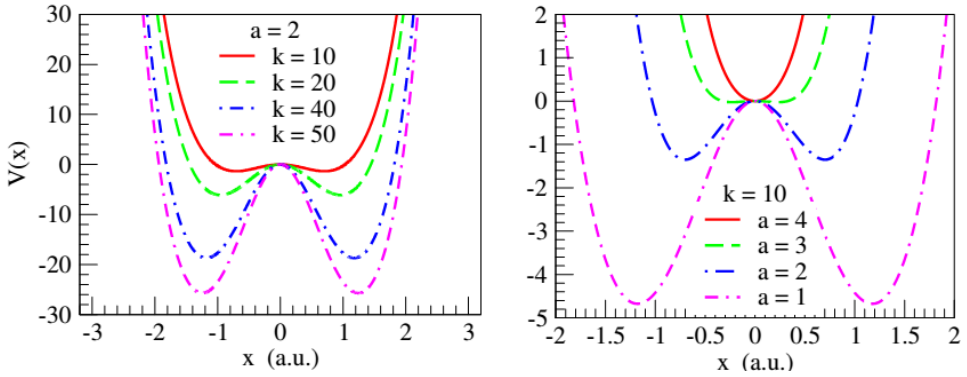

Figure 1 The profile of potential given by Eq. (5) for fixed a with various k (left panel) and for fixed k with various a (righr panel).

Table 1 The calculated 7 lowest energy level (in Ry.) from potential given by Eq. (5), obtained by using $a = 2$ and various k.

	$k = 5$	$k = 10$	$k = 15$	$k = 20$	$k = 25$	$k = 30$
V_{min}	−0.055728090	−1.350889359	−3.508066615	−6.111456180	−9.000000000	−12.09109770
E1	1.393915190	0.370331655	−0.933333951	−2.614961774	−4.721400841	−7.21000273
E2	5.191783643	3.145403569	0.914725044	−1.505566449	−4.111724355	−6.89198492
E3	10.380075438	8.1528209063	6.013253916	4.038265293	2.245335725	0.55071381
E4	16.296137223	13.795247342	11.298251240	8.801886981	6.294444989	3.75765997
E5	22.853954454	20.186925576	17.539244842	14.924841349	12.365071047	9.89147181
E6	29.972872055	27.175030311	24.392131652	21.627804343	18.884834382	16.16435028
E7	37.605130821	34.704925698	31.819199567	28.951170032	26.104776959	23.28521514

Table 1 presents the 7 lowest eigen-energies for potential (5) with $a = 2$ and $k = 5 - 30$, obtained using the filter method. For all k and all energy levels, the filter method produces the same eigen-energies as the analylitical ones. Here, the computational results are presented in 9 decimal places, which, when rounded to 5 decimal places, is exactly the same as the analytical results in Ref. [26]. It can be seen that $V_{\min}$ becomes deeper as k increases. All eigen-energies are located above $V_{\min}$, but can be smaller or greater than $V_{\max} = 0$. As a consequrnce, the eigen-function with $E < V_{\max}$ will experience tunneling. **Table 1** also shows that the energy separation between 2 lowest energy states decreases as k increases.

The eigenfunctions for the ground state and first excited states for potential (5) with $a = 2$ and various k are shown in **Figure 2**, while the eigen-energies are shown in **Table 2**. The numerical eigenfunctions and eigen-energies are in agrement with the analytical ones shown in [26]. It can be seen in the figures that for $k = 10$, the eigenfunction of ground state has no trough at its peak implies absence of tuneellling. As the local maximum $V_{\max} = 0$, absence of the tunelling implies that first eigen-energy is positive, as in the case of single well potential.

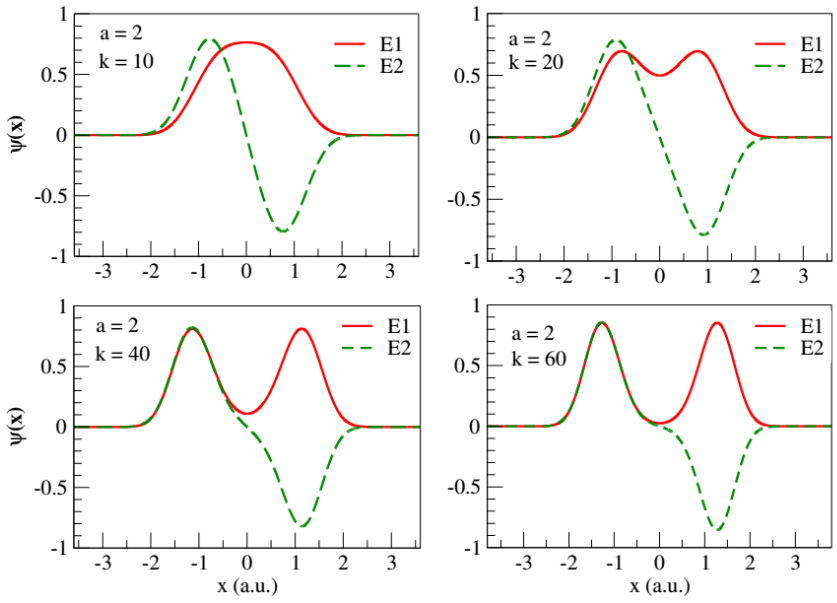

Figure 2 The eigenfunctions for the 2 lowest energy levels for potential (5) with $a = 2$ and various k.

For $k = 15$, the eigenfunction of ground state exhibits a trough at its peak, means that the eigenfunction is experiencing tunneling, and therefore its first eigen-energy is negative. However, the energy of first excited state for $k = 15$ is still postive. For $k = 20$, the eigenfunction of ground state has a deeper trough at its peak, and therefore its first eigen-energy is more negative. Likewise, the energy of the first excited state is also negative. Then we have tunelling case of the 2 lowest energy levels for larger k ($k \geq 20$), and non tunelling case for smaller k ($k < 20$).

For tunelling case, the 2 lowest eigen-energies are smaller than $V_{\max}$ so that the eigenfunction tunells the central potential, where they can be considered as a single energy state undergoing separation. In this case, there is actually one state only, that separate become 2 states due to the potential. The first separation is the symmetric eigenfunction with lower energy and appears as the ground energy state. The other separation is the anti-symmetric eigenfunction with higher energy and appears as the first excited state. **Figure 2** shows that the eigenfunction of the ground state has 2 maxima as a fingerprint of tunelling through central potential in the DWP. Moreover, the first excited state eigenfunction appears as an asymmetric form of the ground state eigenfunction, as an evidence that the 2 energy states can be thought of as splitting energy states. As a separated states, E_2 is closed to E_1. As k increases, the trough depth increases so that the first excited state eigenfunctions become more and more similar to the ground state eigenfunctions, and the energy separation $\Delta E = E_2 - E_1$ becomes smaller, as shown in **Table 2**.

Table 2 The calculated 2 lowest energy level from potential given by Eq. (5), obtained by using $a = 2$ and various k.

k	Present work			Exact [26]	
	E_1 (Ry.)	E_2 (Ry.)	$E_2 - E_1$ (Ry.)	E_1 (Ry.)	E_2 (Ry.)
0	2.226545170	7.066837036	4.840291866	2.22655	7.06684
1	2.071970325	6.704726653	4.632756328	2.07197	6.70473
2	1.911881221	6.336312178	4.424430958	1.91188	6.33631
3	1.745838105	5.961445390	4.215607285	1.74584	5.96145
4	1.573358700	5.579982182	4.006623481	1.57336	5.57998
5	1.393915190	5.191783643	3.797868453	1.39392	1.39392
10	0.370331655	3.145403569	2.775071914	0.370332	3.14540
15	−0.933333951	0.914725044	1.848058995	−0.933334	0.914725
20	−2.614961774	−1.505566449	1.109395325	−2.61496	−1.50557
25	−4.721400841	−4.111724355	0.609676486	−4.7214	−4.11172
30	−7.210002732	−6.891984920	0.318017812	−7.2100	−6.89198
35	−9.992168585	−9.829457106	0.162711479	*n/a*	*n/a*
40	−12.988607873	−12.905375574	0.083232299	*n/a*	*n/a*
45	−16.144497565	−16.101551359	0.042946207	*n/a*	*n/a*
50	−19.424130263	−19.401696468	0.022433794	*n/a*	*n/a*
55	−22.803743558	−22.791864681	0.011878877	*n/a*	*n/a*
60	−26.266763326	−26.260386200	0.006377126	*n/a*	*n/a*

Next, we want to find the dependence of the ground state energy E_1 on k. In **Figure 3** (left panel), we plot the ground state energy E_1 as a function o k. As shown in the figure, it turns out that the ground state energy is a linear function of k, eventhough with different slope $\frac{dE_1}{dk}$ for tunelling and non tunelling case. For non tunelling case, the slope is quite gentle, and become steeper for tunelling case, as follow;

$$E_1 = \begin{cases} -0.4099k + 7.1624 & \text{for non tunelling case} \\ -0.6212k + 11.536 & \text{for tunelling case} \end{cases}. \quad (9)$$

Eq. (9) can be understood from the fact that $V_{\min} = -\left(a - \sqrt{k}\right)^2$ so that for constant a reads $V_{\min} \propto -k$ where for $a = 2$ and $20 \le k \le 60$ we obtain $V_{\min} = -0.6757k + 7.9746$. If the ground state energy has a constant height with respect to $V_{\min}$ regardless k, or $E_1 - V_{\min}$ is constant, then it should be $E_1 \propto k$. The fact that the calculated slope $\frac{dE_1}{dk} = -0.62121$, rather than $\frac{dE_1}{dk} = -0.6757$, indicates the dependence of $E_1 - V_{\min}$ on k.

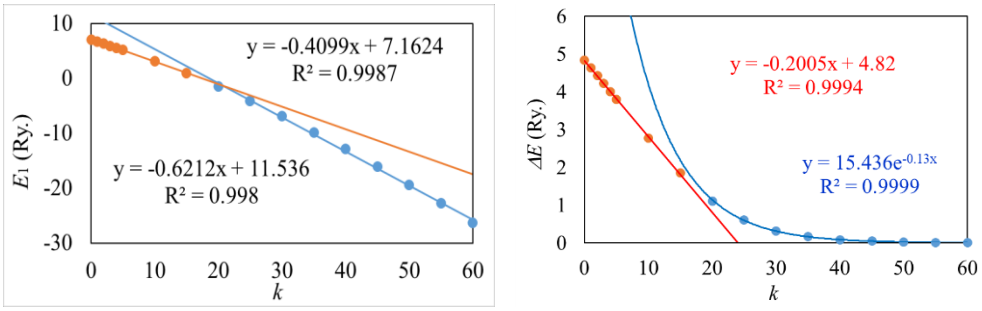

Figure 3 The energy of the ground state (left panel) and energy separation (right panel) as a function of k of potential given by Eq. (5) with $a = 2$ for tunelling states (blue curve) and non-tunelling states (red curve).

In **Figure 3** (right panel), we plot the energy separation between the first exited states and the ground states, $\Delta E = E_2 - E_1$, as a function of k. The figure shows that ΔE is a linier function of k for non tunelling case and an exponential function for tunelling case given by;

$$\Delta E = \begin{cases} -0.2005k + 4.82 & \text{for non tunelling case} \\ 15.436\exp(-0.13k) & \text{for tunelling case} \end{cases}. \tag{10}$$

Eqs. (9) and (10) can be used to estimate the 2 lowest energy levels for potential (5) with $a = 2$ and arbitraty k.

To understand Eq. (10), we recall the aprroximated theoretical results where the energy separation is given by $\Delta E = A\exp(-S/\hbar)$ [40-41]. Here, S is the usual classical action inside the classically forbidden region (between the 2 turning points) $S = \int_{-t}^{t} p(x)dx = \int_{-t}^{t} \sqrt{2m[V(x) - E_m]}dx$ and $A = \frac{\hbar\omega}{\sqrt{e\pi}}$ is called the tunneling amplitude. In the last equation, $V(x)$ is the potential, that for current case is given by Eq. (5) where $V(x) \propto k^2$. E_m is the mid-energy of 2 lowest states given by $E_m = \frac{1}{2}(E_1 + E_2) < 0$. For tunelling case, we obtained that E_m is a linear function of k given by $E_m = -0.5981k + 10.351$ in **Figure 4** (left panel). For tunelling case, a particle with energy E_m penetrates a potential barrier with height of $V_{\max} = V(x = 0) = 0$ and width of $2t$ where t is a point when E_m crosses $V(x)$. As $V(x) \propto k^2$ and $E_m \propto -k$ then it is reasonable to have linear dependence of S on k as shown in **Figure 4** (right panel) and exponential dependence of ΔE on k, as stated in Eq. (10).

We also calculate the dependence of energy separation ΔE on classical action S, where we obtain $\Delta E = 2.5085\exp(-0.45S)$. Note that we obtain the relation $\Delta E = 2.5085\exp(-0.45S)$, violating $\Delta E \propto \exp(-S)$, because of Rydnerg units. It is also possible to calculate the frequency of oscillation by taking $= \frac{\hbar\omega}{\sqrt{e\pi}} = 2.5085$ Ry where we obtain $\omega = 1.47x10^{16}$ rad/s.

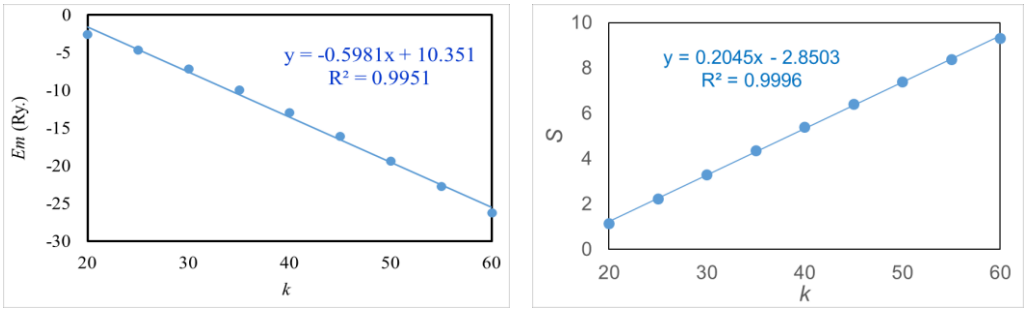

Figure 4 The mid-energy $E_m = \frac{1}{2}(E_1 + E_2)$ (left panel) and classical action S (right panel) of potential given by Eq. (5) for tunelling states as a function k.

Now let's discuss the second potential, given by Eq. (7). The potential profile depicted in **Figure 5** for constant c and various k (left panel) and for constant k and various c (right panel). It exhibits a local maximum at $x_{\max} = 0$ with $V_{\max} = 0$ and 2 symmetric local minima at $x_{\min}$ satisfies $\sinh^6(x) + 2\sinh^4(x) + \sinh^2(x) - \frac{k}{2c^2} = 0$ with $V_{\min} < 0$. It is clear that for the potential (7), the DWP appears for $k > 0$ only, and is more pronounced for larger $\frac{k}{2c^2}$. For $k = 0$, Eq. (7) reduces to a single well potential.

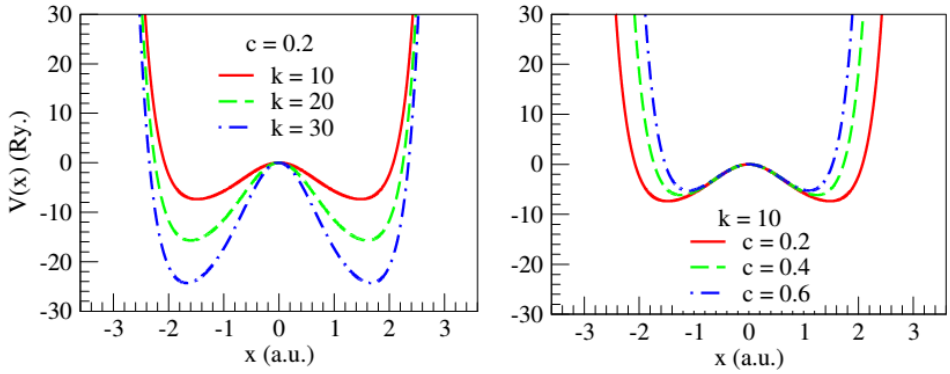

Figure 5 The profile of potential given by Eq. (7) for fixed c with various k (left panel) and for fixed k with various c (righr panel).

Table 3 presents the 7 lowest eigen-energies for potential (7) with $c = 0.2$ and $k = 0 - 30$, obtained using the filter method. For all k values and all energy levels, the filter method produces the same eigen energies as the analytical ones. Here, the computational results are presented in 9 decimal places, which, when rounded to 5 decimal places, is exactly the same as the analytical results [23]. It can be seen that $V_{\min}$ does not appear for $k = 0$ and becomes more negative as k increases. Eigen-energy can be positive or negative, but always greater than $V_{\min}$. It can also be seen from **Table 3** that the distance between energy levels decreases as k increases.

Table 3 The calculated 7 lowest energy level (in Ry.) from potential given by Eq. (7), obtained by using $c = 0.2$ and various *k*.

	$k = 0$	$k = 1$	$k = 5$	$k = 10$	$k = 20$	$k = 30$
V_{min}	-	−0.514033431	−11.500639655	−7.373945617	−15.715581358	−24.310402055
E1	0.619750295	0.299447345	−1.358219687	−4.282107203	−11.530823579	−19.442755217
E2	2.372141929	1.789086128	−0.692081013	−4.081663155	−11.510193831	−19.439853436
E3	5.051387134	4.499848454	2.517582603	0.491457364	−3.962994847	−10.038074192
E4	8.507959397	7.923600949	5.612250801	2.729699778	−3.305941073	−9.900171222
E5	12.660949823	12.062707546	9.712918816	6.919982981	2.182440680	−1.893951088
E6	17.459177917	16.848576697	14.431151523	11.465721511	5.674397199	−0.129116224
E7	22.866136554	22.245906145	19.785214345	16.760703767	10.955712529	5.748924624

The eigen-energies for the ground state and first exited states for potential (7) with $c = 0.2$ and various *k* are shown in **Table 4**, while the eigenfunctions are shown in **Figure 6**. The numerical eigen-energies and eigenfunction are in agrement with the analytical ones shown in [26].

Table 4 The calculated 2 lowest energy level from potential given by Eq. (7), obtained with $c = 0.2$ and barious *k*.

k	Present work			Excat [26]	
	E_1 (Ry.)	E_2 (Ry.)	$E_2 - E_1$ (Ry.)	E_1 (Ry.)	E_2 (Ry.)
0	0.619750295123	2.372141928809	1.752391633685	0.61975	2.37214
1	0.299447345769	1.789086127947	1.489638782178	0.299447	1.78909
2	−0.055305226317	1.190634106237	1.245939332554	−0.0553052	1.19063
3	−0.448340566422	0.577241710449	1.025582276872	−0.448341	0.577242
4	−0.882334435296	−0.050539032325	0.831795402971	−0.882334	−0.050539
5	−1.358219687326	−0.692081012899	0.666138674428	−1.35822	−0.692081
10	−4.282107203422	−4.081663155508	0.200444047915	−4.28211	−4.08166
15	−7.772840695829	−7.711255645316	0.061585050513	−7.77284	−7.71126
20	−11.530823578508	−11.510193830856	0.020629747652	−11.5308	−11.5102
25	−15.437673856027	−15.430188526628	0.007485329398	−15.4377	−15.4302
30	−19.442755210523	−19.439853435757	0.002901774766	−19.4428	−19.4399
35	−23.519731764828	−23.518543581488	0.001188183341	*n/a*	*n/a*
40	−27.652720347101	−27.652210947592	0.000509399509	*n/a*	*n/a*
45	−31.831152591695	−31.830998540057	0.000154051639	*n/a*	*n/a*
50	−36.047509072401	−36.047404309373	0.000104763028	*n/a*	*n/a*

From **Figure 6** it can be seen that there is no tunneling for $k = 1$ or $E_1 > V_{\max}$ and therefore the eigenfunction of ground state has no trough at its peak, as in the case of single well potential. For $k = 5$, tunelling has occurred or $E_1 < V_{\max}$, but the eigenfunction of first excited state is not yet seen as an asymmetrical form of the symmetric eigenfunction of ground state. For $k \geq 10$, tunneling has occurred or $E_1 < V_{\max}$ and the eigenfunction of first excited state is an asymmetrical form of the symmetric eigenfunction of ground state. It implies that E_2 is closed to E_1 and the energy separation $\Delta E = E_2 - E_1$ is small. As *k* increases ΔE becomes smaller, as shown in **Table 4**.

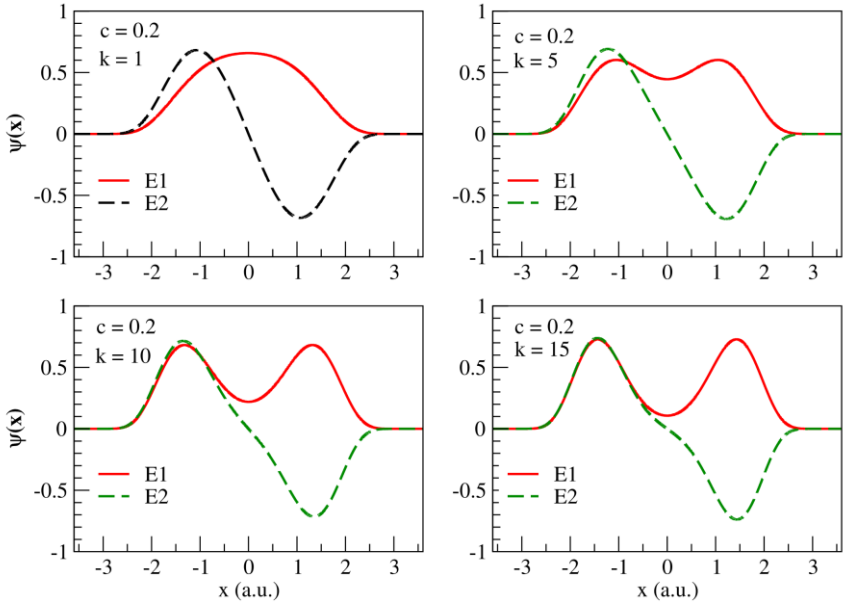

Figure 6 The eigenfunction of the 2 lowest energy level of potential (7) with constant $c = 0.2$ and various k.

In **Figure 7** (left panel), we plot the ground state energy E_1 as a function of k. As shown in the figure, it turns out that the ground state energy is a linear function of k, eventhough the tunelling case has greater slope $\frac{dE_1}{dk}$, as follow;

$$E_1 = \begin{cases} -0.3951k + 0.6836 & \text{for non tunelling case} \\ -0.7985k + 4.2321 & \text{for tunelling case} \end{cases}. \tag{11}$$

To estimate the 2 lowest energy sates, we need the dependence of energy separation ΔE on DWP parameter k, which according to **Figure 7** (right panel), is given by;

$$\Delta E = \begin{cases} -0.2179k + 1.7132 & \text{for non tunelling case} \\ 0.8091\exp(-0.19k) & \text{for tunelling case} \end{cases}. \tag{12}$$

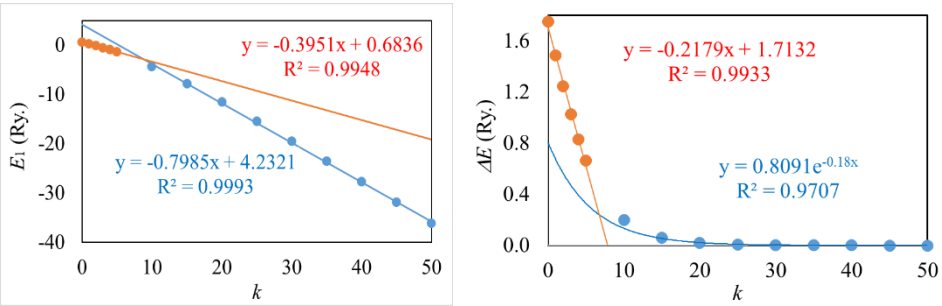

Figure 7 The energy of the ground state (left panel) and energy separation (right panel) as a function of k of potential given by Eq. (7) with $c = 0.2$ for tunelling states (blue curve) and non-tunelling states (red curve).

From the 2 potentials investigated, it was found that the 2 energy states can be considered as energy separation if the following 2 conditions are met. First, the 2 states of separation energy are lower than the

potential barrier peaks. Second, the wave function of the 2 energy levels is a symmetric and antisymmetric wave pair. In this case, energy separation is an exponential function of the DPW parameter.

Finally, it is important to investigate whether Eqs. (11) and (12) hold for any tunneling case, regardless of the DWP parameter, energy level, and DWP model. To overcome the first issue, we perform calculations for the 2 lowest energy level for potential given by Eq. (7) but $c = 0.4$ and variation k, and analyze the results, as shown in **Figure 8**. We find that the applicability of Eqs. (11) and (12) are independent of the DWP parameter.

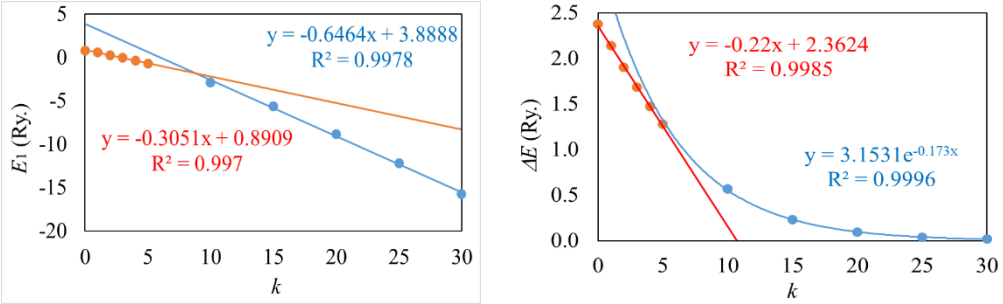

Figure 8 The first energy E_1 (left panel) and energy separation $\Delta E = E_2 - E_1$ (right panel) for potential given by Eq. (7) with $c = 0.4$ as a function of k, for tunelling states (blue curve) and non-tunelling states (red curve).

To overcome the second issue, we perform calculations for E_3 and E_4 of potential given by Eq. (7), with the same $c = 0.2$ and various k, and analyze the results, as shown in **Figure 9**. Like ΔE_{12}, in the tunnel region we find that ΔE_{34} is also an exponential function of k. The only difference occurs in the non-tunneling region, where ΔE_{34} is a quadratic function of k, while ΔE_{12} is a linear function of k. Regarding the last issue, we perform calculations for the 2 lowest energy levels for RBP and find that Eqs. (11) and (12) hold. These results will be published in a separate paper.

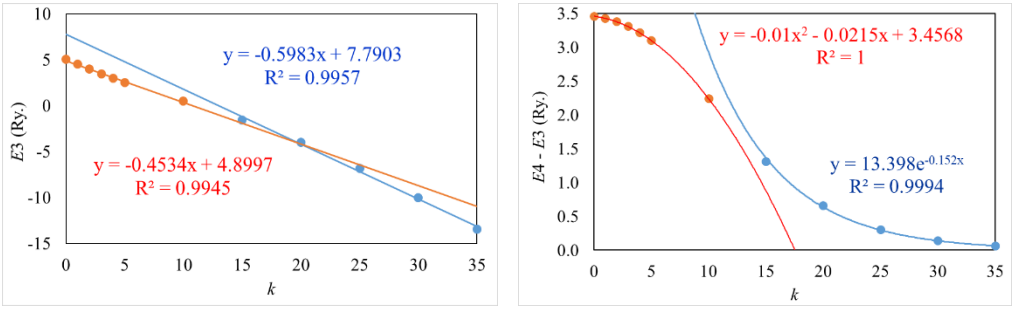

Figure 9 The third energy E_3 (left panel) and energy separation $\Delta E_{34} = E_4 - E_3$ (right panel) for potential given by Eq. (7) with $c = 0.2$ as a function of k, for tunelling states (blue curve) and non-tunelling states (red curve).

Conclusions

In conclusion, we succeeded in obtaining accurate eigen-energies and eigenfunctions for the hyperbolic-symmetric DWP class using the Filter method. The calculation results are in accordance with the exact analytical results obtained using the Heun's confluent function. For large k, the 2 lowest eigen-energies are smaller than V_{max}, so that the eigenfunction tunells the central potential, where they can be considered as a single energy state undergoing separation. In this case, the symmetric eigenfunction has lower energy and appears as the lowest energy level, while the antisymmetric eigenfunction has higher energy and appears as the first excited state. The energy separation $\Delta E = E_2 - E_1$ is an exponential function of k, while the lowest energy is a linear function of k. This relationship allows one to estimate the 2 lowest energy levels. The exponential dependence of ΔE on k agrees with the theoretical approximation, which is shown by the linear relationship between k and the classical action in the classical forbidden region S.

Acknowledgements

This work was financially supported by Faculty of Mathematics and Natural Sciences Brawijaya University in Indonesia, through "Research of DPP/SPP year 2023" with the contract number: 2824.28/UN10.F09/PN/2023.

References

[1] CC Win. Symmetrical double-well potential and its application. *Mandalay Univ. Res. J.* 2018; **9**, 1.
[2] AE Sitnitsky. Exactly solvable double-well potential in Schrödinger equation for inversion mode of phosphine molecule. *Comput. Theor. Chem.* 2021; **1200**, 113220.
[3] T Novoa, J Contreras-García, P Fuentealba and C Cárdenas. Aspects of electronic bonding under pressure: Electron localization in symmetric double well model. *J. Chem. Phys.* 2019; **150**, 2043.
[4] J Adriazola, R Goodman and P Kevrekidis. Efficient manipulation of bose-einstein condensates in a double-well potential. *Comm. Nonlinear Sci. Numer. Simulat.* 2023; **122**, 107219.
[5] F Theel, K Keiler, SI Mistakidis and P Schmelcher. Many-body collisional dynamics of impurities injected into a double-well trapped Bose-Einstein condensate. *Phys. Rev. Res.* 2021; **3**, 023068.
[6] CM Porto and NH Morgon. Analytical approach for the tunneling process in double well potentials using IRC calculations. *Comput. Theor. Chem.* 2020; **1187**, 112917.
[7] C Fábri, R Marquardt, AG Császár and M Quack. Controlling tunneling in ammonia isotopomers. *J. Chem. Phys.* 2019; **150**, 014102.
[8] Y Yao and J Ma. Logical chaotic resonance in a bistable system. *Int. J. Bifurcat. Chaos* 2020; **30**, 2050196.
[9] Y Shah, I Kapoor, P Singhvi, B Birua and R Parekh. Simulation and comparative study of resonant tunneling diode. *Trends Sci.* 2022; **19**, 5615.
[10] W Belaid1, HE Ghazi, R En-Nadir, HŞ Kılıç, I Zorkani and A Jorio. Temperature-related electronic low-lying states in different shapes $In_{.1}Ga_{.9}N$/GaN double quantum wells under size effects. *Trends Sci.* 2022; **19**, 5777.
[11] M Razavy. A model for diffusion in a bistable potential field. *Phys. Lett.* 1979; **72**, 89-90.
[12] H Konwent. One-dimensional Schrödinger equation with a new type double-well potential. *Phys. Lett.* 1986; **118**, 467-70.
[13] S Habib, A Khare and A Saxena. Statistical mechanics of double sinh-gordon kinks. *Phys. Nonlinear Phenom.* 1998; **123**, 341-56.
[14] AS Durmuslar, CA Billur, A Turkoglu and F Ungan. Optical properties of a GaAs quantum well with new type of hyperbolic confinement potential: Effect of structure parameters and intense laser field. *Optic. Comm.* 2021; **499**, 127266.
[15] H Dakhlaoui, W Belhadj, MO Musa and F Ungan. Electronic states and optical characteristics of GaAs spherical quantum dot based on Konwent-like confiing potential: Role of the hydrogenic impurity and structure parameters. *Optik* 2023; **277**, 170684.
[16] H Dakhlaoui, W Belhadj, F Ungan and NS Al-Shameri. Linear and nonlinear optical properties in GaAs quantum well based on Konwent-like potential: Effects of impurities and structural parameters. *Phys. E Low Dimensional Syst. Nanostructures* 2023; **152**, 115760.
[17] AS Durmuslar. Investigation on nonlinear optical properties of symmetric and asymmetric double V-shaped $Al_xGa_{1-x}As$/GaAs potential wells with structural parameters and external electromagnetic fields. *Philos. Mag*. 2023; **103**, 872-91.
[18] A Turkoglu, H Dakhlaoui, ME Mora-Ramosdan and F Ungan. Optical properties of a quantum well with Razavy confinement potential: Role of applied external fields. *Phys. E Low Dimensional Syst. Nanostructures* 2021; **134**, 114919.
[19] H Dakhlaoui, JA Gil-Corrales, AL Morales, E Kasapoglu, A Radu, RI Restrepo, V Tulupenko, JA Vinasco, ME Mora-Ramosand and CA Duque. Theoretical study of electronic and optical properties in doped quantum structures with Razavy confning potential: Effects of external felds. *J. Comput. Electron.* 2022; **21**, 378-95.
[20] M Gambhir, B Vidhani, S Devi and V Prasad. Impact of asymmetry of Razavy-type coupled well system and static electric field on the time-dynamical studies of entanglement. *Eur. Phys. J. Plus* 2023; **138**, 57.
[21] EB Al, E Kasapoglu, H Sari and I Sökmen. Optical properties of spherical quantum dot in the presence of donor impurity under the magnetic feld. *Phys. B Condens. Matter.* 2021; **613**, 41287.
[22] M Baradaran and H Panahi. Exact solutions of a class of double-well potentials: Algebraic bethe ansatz. *Adv. High Energ. Phys.* 2017; **2017**, 8429863.

[23] AM Ishkhanyan and AE Grigoryan. Fifteen classes of solutions of the quantum two state problem in terms of the confluent Heun function. *J. Phys. Math. Theor.* 2014; **47**, 465205.
[24] Q Dong, G-H Sun, MA Aoki, CY Chen and SH Dong. Exact solutions of a quartic potential. *Mod. Phys. Lett.* 2019; **34**, 1950208.
[25] R Budaca. Quasi-exact solvability of the d-dimensional sextic potential in terms of truncated bi-confluent Heun functions. *Ann. Acad. Rom. Scientists* 2020; **12**, 87-98.
[26] Q Dong, GH Sun, J Jing and SH Dong. New findings for two new type sine hyperbolic potentials. *Phys. Lett.* 2019; **383**, 270-5.
[27] XH Wang, CY Chen, Y You, FL Lu, DS Sun and SH Dong. Exact solutions of the Schrödinger equation for a class of hyperbolic potential well. *Chin. Phys. B* 2022; **31**, 040301.
[28] Q Dong, FA Serrano, GH Sun, J Jing and SH Dong. Semi-exact solutions of the razavy potential. *Adv. High Energ. Phys.* 2018; **2018**, 06426.
[29] S Dong, Q Dong, GH Sun, S Femmam and SH Dong. Exact solutions of the razavy cosine type potential. *Adv. High Energ. Phys.* 2018; **2018**, 5824271.
[30] Q Dong, SS Dong, E Hernández-Márquez, R Silva-Ortigoza, GH Sun and SH Dong. Semi-exact solutions of konwent potential. *Comm. Theor. Phys.* 2019; **71**, 231.
[31] GH Sun, Q Dong, VB Bezerra and SH Dong. Exact solutions of an asymmetric double well potential. *J Math. Chem.* 2022; **60**, 605-12.
[32] Q Dong, HIG Hernández, GH Sun, M Toutounji and SH Dong. Exact solutions of the harmonic oscillator plus non-polynomial interaction. *Proc. Math. Phys. Eng. Sci.* 2020; **476**, 20200050.
[33] GH Sun, CY Chen, H Taud, C Yáñez-Márquez and SH Dong. Exact solutions of the 1D Schrödinger equation with the Mathieu potential. *Phys. Lett.* 2000; **384**, 126480.
[34] KI Kowari. A numerical analysis of motion in symmetric double-well harmonic potentials using pseudospectral methods. *Chem. Phys. Lett.* 2020; **739**, 136941.
[35] AJ Sous. Eigenenergies for the razavy potential using the asymptotic iteration method. *Mod. Phys. Lett.* 2007; **22**, 1677-84.
[36] X Wang, J Kou and H Gao. Linear energy stable and maximum principle preserving semi-implicit scheme for allen-cahn equation with double well potential. *Comm. Nonlinear Sci. Numer. Simulat.* 2021; **98**, 105766.
[37] FG Montoya and S Wiggins. Revealing roaming on the double Morse potential energy surface with Lagrangian descriptors. *J. Phys. Math. Theor.* 2020; **53**, 235702.
[38] R Santana-Carrillo, JMV Peto, GH Sun and SH Dong. Quantum information entropy for a hyperbolic double well potential in the fractional Schrödinger equation. *Entropy* 2023; **25**, 988.
[39] JP Killingbeck, G Jolicard and A Grosjean. The hill determinant method revisited. *J. Math. Chem.* 2019; **57**, 107-18.
[40] A Garg. Tunnel splittings for one-dimensional potential wells revisited. *Am. J. Phys.* 2000; **68**, 430-7.
[41] AE Sitnitsky. Analytic calculation of ground state splitting in symmetric double well potential. *Comput. Theor. Chem.* 2018; **1138**, 15-22.
[42] M Nurhuda and A Rouf. Filter method without boundary-value condition for simultaneous calculation of eigenfunction and eigenvalue of a stationary Schrödinger equation on a grid. *Phys. Rev. E* 2017; **96**, 033302.
[43] Abdurrouf, M Nurhuda and Wiyono. Modelling one-dimensional crystal by using harmonic oscillator potential. *IOP Conf. Ser. Mater. Sci. Eng.* 2019; **546**, 052001.
[44] Abdurrouf, MA Pamungkas, W Wiyono and M Nurhuda. Implementation of filter method to solve the Kronig-Penney model. *AIP Conf. Proc.* 2020; **2234**, 040001.
[45] Abdurrouf, MA Pamungkas and M Nurhuda. The energy spectrum of imperfect kronig-penney model. *Int. J. Innovat. Tech. Exploring Eng.* 2020; **9**, 2278-3075.
[46] Abdurrouf, MA Pamungkas and M Nurhuda. Numerical solution of the schrödinger equation with periodic coulomb potential. *J. Phys. Conf. Ser.* 2021; **1825**, 012105.